VII International Conference on Computational Methods for Coupled Problems in Science and Engineering
COUPLED PROBLEMS 2017
M. Papadrakakis, E. Oñate and B. Schrefler (Eds)

A FLUID-STRUCTURE SOLVER FOR CONFINED MICROCAPSULE FLOWS

B. Sarkis*†, A.-V. Salsac* and J.-M. Fullana†

*Laboratoire BioMécanique et BioIngénierie (UMR CNRS 7338)
Université de Technologie de Compiègne, CNRS, Sorbonne Universités
CS60319, 60203 Compiègne, France
e-mail: a.salsac@utc.fr - web page: http://www.utc.fr/bmbi/

†Institut Jean Le Rond ∂'Alembert (UMR CNRS 7190)
Université Pierre et Marie Curie, CNRS, Sorbonne Universités
4 place Jussieu, 75252 Paris CEDEX, France
e-mail: jose.fullana@upmc.fr - web page: http://www.dalembert.upmc.fr/

Key words: Microcapsules, Fluid-Structure Interaction, Confined Environment, Finite Volumes, Finite Elements, Immersed Boundary Method.

Abstract. We present a fluid-structure coupling method designed to study capsules flowing in a confined environment. The fluid solver is based on the Finite Volume Method and is coupled to a Finite Elements solid solver using the Immersed Boundary Method. We study the relaxation of a spherical capsule, initially deformed into an ellipsoid, and released in a square cross-section channel within a quiescent fluid environment. We perform a convergence study in order to validate the numerical method and consider the effect of the inertial forces on the capsule relaxation.

1 INTRODUCTION

Encapsulation consists in protecting a substance from the surrounding medium with a solid or flexible envelope. One of the main goals of encapsulation is the transport of the substance and the control of its release, whether it is to be prevented or operated at a desired location or rate [1]. Understanding the capsule dynamics provides the possibility to better control the potential release of the inner substance. Flexible capsules find applications in various fields, particularly in biomedical areas (e.g. targeted drug delivery) and food industry. Over the last decades, the flow around flexible capsules and the resulting fluid-structure interactions have been studied experimentally [2, 3, 4], analytically [5, 6] as well as numerically [7, 8]. Small scale experimental setups can provide results in various confined geometries and flow configurations, but the observations are complex due to the scale of the microparticles. Analytical calculations give comprehensive

accurate results but are restricted to simple flow configurations and small deformations of the capsule shape. The advantage of numerical simulations is that they provide a good approximation of quantities that are inacessible through experimental measurement (e.g. membrane tension) and that would be difficult to model analytically (e.g. capsules flowing in complex geometries). They can also simulate a wide range of properties for the flow and capsule, and parameters for the case studied. The fluid-structure interactions of the capsule wall deformation with the internal and surrounding fluid flows can be modeled choosing between two approaches to treat the capsule and the fluids: Lagrangian or Eulerian. The different existing fluid-structure solvers can thus be classified in three groups: fully Lagrangian, fully Eulerian and the mixed Eulerian-Lagrangian. Among the fully Lagrangian approaches, one can mention the Boundary Integral Method [7], which is very precise, computationnaly efficient and robust but only applicable to Stokes flow. On the other hand, fully Eulerian methods comprise the level-set method and Volume Of Fluids (VOF) methods. The latter have the drawback of interface reconstruction, which is hardly compatible with a continuous mapping. The level-set method is a relevant choice: despite the fact that early implementations were neither able to conserve the fluid enclosed mass [9] nor to treat the membrane elastic behaviors, these issues have been solved since then [10]. Finally, the mixed Eulerian-Lagrangian approaches include the Immersed Boundary Method (IBM) [11, 12], which is very popular thanks to its extreme simplicity of implementation. It has the drawback of being typically unstable with stiff membranes but this issue has been recently solved [13]. It is, however, stable in the case of flexible membranes, but capsule flow simulations in complex confined geometries remain challenging [13]. Our aim is to develop a tool able to compute the fluid-structure interactions in confined geometries at potentially non-zero Reynolds numbers. The finite elements solver of Caps3D [7] is coupled with the open-source finite volume solver Basilisk that has been designed to solve multiphase flows [14]. The objective of the present paper is to validate the numerical code by considering the relaxation of a pre-deformed capsule within a confined environment.

2 PROBLEM STATEMENT

We consider an initially spherical capsule of radius a placed in a square cross-section channel of length L and half-width l (Figure 1). Let O be the center of the channel and x the coordinate along the centerline longitudinal axis of the channel, so that it defines the axis O_x. Let y and z be the two other (transversal) coordinates. We respectively call S_i, S_o and S_l the inlet, outlet and (four) lateral sections, the latter being the walls of the channel. The capsule is constituted of a membrane enveloping an internal fluid. The internal and surrounding fluids have the same density ρ and the same viscosity μ. The capsule membrane surface shear modulus is G_s (Figure 1). We neglect the wall thickness and model the capsule wall as a 2D membrane. We thus neglect bending effects. The objective of the fluid-structure solver will be to study the dynamical flow of the capsule flowing in the channel under an average inlet flow velocity $V = 0.05\frac{G_s}{\mu}$. We use as physical

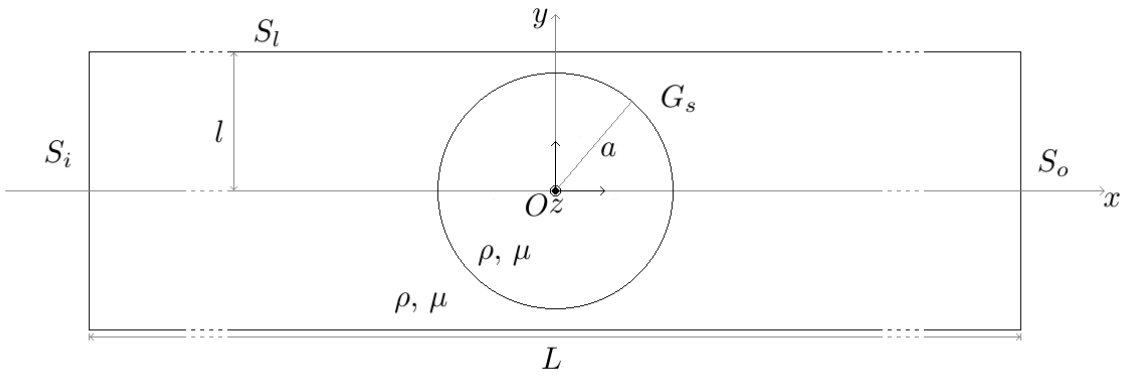

Figure 1: Schematic of the framework. A spherical capsule of radius a and surface shear modulus G_s is placed in a square cross-section chanel of length L and half-width l. The fluid inside and outside the capsule both have a density ρ and a viscosity μ.

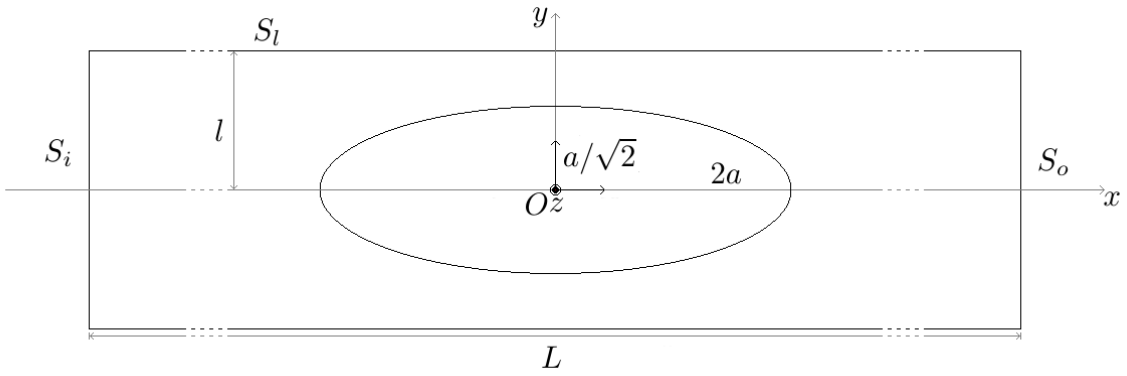

Figure 2: Scheme of the validation case: a spherical capsule of radius a is pre-deformed into an ellipsoid of axes $(2a, a/\sqrt{2}, a/\sqrt{2})$ in a square cross-section channel of length L and half-width l. The half-great axis is along O_x and the half-small axes are in the yOz plane.

kinematic scales l to non-dimensionalize the lengths and $T_V = l/V$ to non-dimensionalize time. The dimensionless coordinates are $x' = x/l$, $y' = y/l$, $z' = z/l$, $t' = t/T_V$. The scale used to non-dimensionalize the forces is $\rho V^2 l^2$. The capsule motion and deformation are governed by the two following dimensionless numbers: the capsule-to-channel size ratio $\frac{a}{l}$ and the Reynolds number $Re = \frac{\rho V l}{\mu}$, which is the ratio of the inertial to viscous forces. For the sake of simplicity, in the following the prime symbols are omitted. To validate the code, we will consider the relaxation of a capsule pre-deformed into an ellipsoid of half-great axis $2a$ along O_x and half-small axes $a/\sqrt{2}$ (Figure 2). In this case, the velocity field is induced by the elastic deformation of the capsule. It is placed at time $t = 0$ at the center of the channel (the capsule center of mass being at O) in a fluid at rest.

3 NUMERICAL METHODS

3.1 Meshing of the capsule and fluid domains

Triangular second-order finite elements are used to mesh the capsule wall. Let $\mathcal{L}$ be the Lagrangian configuration, which is the set of the Lagrangian nodes $\underline{X} = (X_x, X_y, X_z)$ at time t. The meshing $\mathcal{L}$ is built iteratively from an icosahedron [7]. The typical Lagrangian mesh size is h. Two different values of h are considered here: $h = 0.039$ and $h = 0.02$, corresponding respectively to 10 242 and 40 962 Lagrangian nodes ($\text{card}(\mathcal{L}) \in \{10\,242; 40\,962\}$). The mesh size $h = 0.078$ has also been tested but the mesh is found to be too coarse to provide good results. The fluid domain is meshed with a Eulerian regular cartesian grid. Let $\mathcal{E}$ be the set of the Eulerian cubical mesh centers (x, y, z). The non-dimensionalized length of the channel is set to $L = 8$. The Eulerian mesh size is fixed and set to be $\Delta x = 1/32 = 0.03125$. The number of Eulerian meshes is 1 048 576 ($\text{card}(\mathcal{E}) = 1\,048\,576$)). The mesh size $\Delta x = 1/16 = 0.0625$ has also been tested but is not presented here because it is too coarse to provide precise results. Four integration timesteps are considered: $dt = 10^{-3}$, $dt = 5 \times 10^{-4}$, $dt = 2 \times 10^{-4}$ and $dt = 10^{-4}$.

3.2 Membrane equilibrium equations

The membrane solver code, Caps3D, uses the Lagrangian configuration $\mathcal{L}$ to compute the non-dimensionalized Cauchy tension tensor $\underline{\underline{T}}$, which provides the non-dimensionalized tension (lineic force) $\underline{\tau}$ exerted in a direction $\underline{n}$ by $\underline{\tau}(\underline{n}) = \underline{\underline{T}}.\underline{n}$. This tensor is calculated using the strain energy function w_s describing the material constitutive law. In the present study we model the capsule behavior using the Skalak et al. law [15]. For this law, the non-dimensionalized surface energy w_s is given by:

$$w_s = \frac{1}{4}\left(I_1^2 + 2I_1 - 2I_2 + CI_2^2\right), \tag{1}$$

where C is a constant parameter that relates the surface shear modulus G_s and surface area dilatation modulus of the capsule. I_1 and I_2 are the first and second strain invariants of the surface evolution. The Skalak et al. law is particularly adapted to model the strain-hardening behavior of cells, such as red blood cells which have a quasi surface-incompressible membrane (C¿¿1). The surface load $\underline{q}$ exerted by the fluid on the membrane is given by the membrane equilibrium law

$$\underline{\nabla_s}.\underline{\underline{T}} + \underline{q} = \underline{0}. \tag{2}$$

By the action-reaction principle, $-\underline{q}$ is the surface load exerted by the membrane on the fluid. More details may be found in [7, 15].

3.3 Fluid dynamics equations

The fluid equations are solved over the Eulerian grid $\mathcal{E}$ by the open-source code, Basilisk. In order to compute the Eulerian velocity field, Basilisk [14] uses the incom-

pressible ($\underline{\nabla}.\underline{v} = 0$), three-dimensional Navier-Stokes equations

$$\frac{\partial \underline{v}}{\partial t} + (\underline{v}.\underline{\nabla})\underline{v} = -\underline{\nabla} p + \frac{1}{Re}\underline{\Delta u} + \underline{f}, \tag{3}$$

where $\underline{v} = (v_x, v_y, v_z)$ is the fluid velocity, $\rho = \rho(x, y, z, t)$ the fluid density and $\mu = \mu(x, y, z, t)$ the dynamic viscosity. The Navier-Stokes equations are solved using a finite volume approach based on a projection method [16]. For Stokes flows, the non-linear term $(\underline{v}.\underline{\nabla})\underline{v}$ is set to zero. The spatial discretization is done using a octree cubic cell allowing dynamic grid refinement in the lubrication film. The source-term $\underline{f}$ is the volumic force exerted by the capsule on the fluid. Finally, the boundaries are that of a fluid at rest. Basilisk uses Dirichlet and Neumann boundary conditions. For the speed $\underline{v}$ we set a zero Dirichlet boundary condition on the inlet and lateral sections (S_i and S_l) and a zero Neumann boundary condition on the outlet section S_o. Additional optional boundaries are set for the pressure p: a zero Neumann condition on S_i and a zero Dirichlet condition on S_o [16].

3.4 Coupling strategy and method

The coupling strategy is based on the Immersed Boundary Method [11]. At each timestep:

- the forces are transmitted from the capsule membrane to the fluid as source-terms.
- the membrane capsule is advected by the fluid towards a new configuration.

The surface elastic load $\underline{q}$ is converted to fluid source-term volume forces $\underline{f}$ using the following two steps:

- the surface load $-\underline{q}$, defined at each $\underline{X} \in \mathcal{L}$, is first integrated into a ponctual force $\underline{F}(\underline{X})$. This integration is made using a 3 Hammer point scheme. This guarantees the force conservation over each finite element.
- the ponctual force $\underline{F}(\underline{X})$ is then spread into the source-term volumic force $\underline{f}$ by the immersed boundary method. We use the classical cosine immersed boundary filter δ_c [11]:

$$\underline{f}(x, y, z) = \sum_{\underline{X}=(X_x, X_y, X_z)\in\mathcal{L}} \frac{\underline{F}(\underline{X})}{(\Delta x)^3} \delta_c\left(\frac{x - X_x}{\Delta x}\right) \delta_c\left(\frac{y - X_y}{\Delta x}\right) \delta_c\left(\frac{z - X_z}{\Delta x}\right), \tag{4}$$

where

$$\forall s \in \mathbb{R}, \delta_c(s) = \frac{1}{4}\left(1 + \cos\left(\frac{\pi s}{2}\right)\right) \mathbb{I}_{|s|\leq 2}. \tag{5}$$

This filter is theoretically of order 1 [12] but is found to be of an order between 1 and 2 in practice.

The volumic force $\underline{f}$ is injected into equation (3), which is solved to provide the new velocity field $\underline{v}(t+dt)$ and update the position of the capsule nodes:

$$\frac{\underline{X}(t+dt)-\underline{X}(t)}{dt}=\sum_{(x,y,z)\in\mathcal{E}}\frac{\underline{v}(x,y,z,t+dt)}{(\Delta x)^3}\delta_l\left(\frac{x-X_x}{\Delta x}\right)\delta_l\left(\frac{y-X_y}{\Delta x}\right)\delta_l\left(\frac{z-X_z}{\Delta x}\right), \tag{6}$$

where

$$\forall s\in\mathbb{R},\delta_l(s)=(1-|s|)\,\mathbb{I}_{|s|\leq 1}. \tag{7}$$

This filter is of order 2 [12].

3.5 Parameters of the problem

The physical parameters are chosed to model an artificial microcapsule released in the tube:

- Capsule-to-channel size ratio $a/l=0.85$;
- Skalak law with $C=1$.

3.6 Criteria to be observed

3.6.1 Convergence study criteria

The criteria for the convergence at the final time $t=10$ of the simulation are:

- the maximum error norm over $\mathcal{L}$ of the difference of the position $\underline{X}$ for the timestep dt of the considered simulation to that obtained with the smallest integration timestep $dt_{\min}=10^{-4}$:

$$N_\infty=\|\underline{X}_{dt}-\underline{X}_{dt_{\min}}\|_\infty=\max_{\underline{X}\in\mathcal{L}}\|\underline{X}_{dt}-\underline{X}_{dt_{\min}}\| \tag{8}$$

- the maximum norm over $\mathcal{E}$ of the difference of the fluid speed to its theoretical value at $t=+\infty$. In this asymptotical state, the relaxation is over and the fluid is at rest. Thus, the criterion becomes:

$$v_{\max}=\|\underline{v}\|_\infty=\max_{(x,y,z)\in\mathcal{E}}\|\underline{v}(x,y,z)\| \tag{9}$$

- the relative membrane surface difference between the Lagrangian configuration $\mathcal{L}$ and the reference spherical shape $\mathcal{L}_0$: $\frac{d\mathcal{S}_\mathcal{L}}{\mathcal{S}_{\mathcal{L}_0}}=\frac{\mathcal{S}_\mathcal{L}-\mathcal{S}_{\mathcal{L}_0}}{\mathcal{S}_{\mathcal{L}_0}}$, where $\mathcal{S}_{\mathcal{L}_0}=4\pi a^2$
- the relative membrane volume difference between the Lagrangian configuration $\mathcal{L}$ and the reference spherical shape $\mathcal{L}_0$: $\frac{d\mathcal{V}_\mathcal{L}}{\mathcal{V}_{\mathcal{L}_0}}=\frac{V_\mathcal{L}-\mathcal{V}_{\mathcal{L}_0}}{\mathcal{V}_{\mathcal{L}_0}}$, where $\mathcal{V}_{\mathcal{L}_0}=\frac{4}{3}\pi a^3$. This variation is an error, since it should be zero.

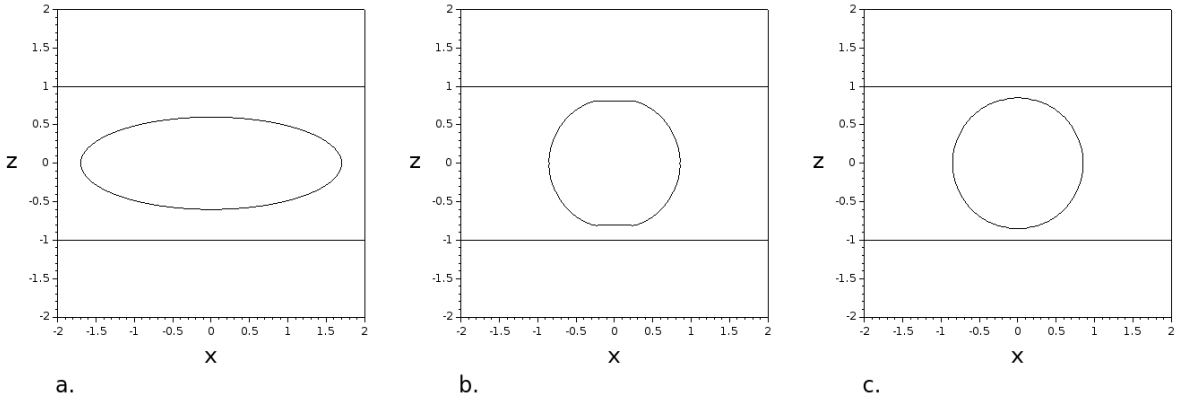

Figure 3: Shape evolution of the capsule relaxing in the channel at $t = 0$ (a), $t = 5$ (b), and $t = 10$ (c) for $h = 0.039$ and $dt = 5 \times 10^{-3}$ in Stokes flow.

3.6.2 Transient state study criteria

During the transient state i.e. $t \in]0, 10[$, the characterization can be done with the parameters of the inertia ellipsoid ϵ of $\mathcal{L}$. The Taylor parametrer is defined by $D_{1,2} = (L_x - L_y)/(L_x + L_y)$, where L_x and L_y are respectively the half-great and half-small axis of ϵ. Under Stokes flow, this approximation is valid: even though the capsule is influenced by the confinement, its shape $\mathcal{L}$ remains roughly ellipsoidal during the transient state (Figure 3). On the contrary, under inertial flow conditions (i.e. solving the full Navier-Stokes equations), the shape is too different from being ellipsoidal. We propose to replace the $D_{1,2}$ parameter with a parameter $\tilde{D}_{1,2} = (\tilde{L}_x - \tilde{L}_y)/(\tilde{L}_x + \tilde{L}_y)$, where $\tilde{L}_x = \max_L(X_x) - \min_L(X_x)$ and $\tilde{L}_y = \max_L(X_y) - \min_L(X_y)$ are the differences of the extremal coordinates of the Lagrangian grid respectively along O_x and O_y. This new definition allows negative values for $\tilde{D}_{1,2}$. For the sake of simplicity, in the following this new parameter is also called "Taylor parameter".

4 RESULTS

4.1 Generalities

The capsule relaxes to its reference spherical geometry. Figure 3 shows the time evolution of the capsule shape for $h = 0.039$ and $dt = 5 \times 10^{-3}$ in Stokes flow. At time $t = 5$ one sees that the capsule shape is influenced by the walls of the channel, the capsule wall becoming parallel to it.

4.2 Final time results

When comparing the capsule shape $\mathcal{L}$ at time t to $\mathcal{L}_0$, we see that the infinite norm $\|\underline{X} - \underline{X_0}\|_\infty$ has an order of magnitude $\sim 1\%$, depending on the Lagrangian mesh size h and time step dt. It is consistent with the evolution of $\mathcal{L}$ towards $\mathcal{L}_0$ over time. Since the final time $t = 10$ is far from the end of the relaxation process which is infinite, the

relaxation is uncomplete and this infinite norm is minorated over $(h, \Delta x, dt) \in (\mathbb{R}^{+,*})^3$ by some constant $K > 0$. Figure 4 presents the values of the 4 criteria defined in subsection 3.6.1. The same orders of magnitude are obtained for the four criteria: they lie between $\sim$0.1% and $\sim$1% for N_∞ (4.a), $v_{\max}$ (4.b), $\frac{d\mathcal{S}_\mathcal{L}}{\mathcal{S}_{\mathcal{L}_0}}$ (4.c) and $\frac{d\mathcal{V}_\mathcal{L}}{\mathcal{V}_{\mathcal{L}_0}}$ (4.d):

- Values of (4.a) prove that the error of convergence has an order of magnitude $\sim 0.1\%$ for the smallest timestep $dt_{\min} = 10^{-4}$;
- Values of (4.b) show that the fluid is almost at rest, but not totally because the final time is $(t = 10)$;
- Values of (4.c) show that the area of $\mathcal{L}$ always differ by less than 1% from that of the reference shape $\mathcal{L}_0$;
- Values of (4.d) show that the volume conservation error is always clearly lower than 1%. They are of the same order or smaller than those obtained by Caroll and Gupta [17]. In the best case, the error is 0.02%, which is indeed much better than [17].

We observe the following effects of the numerical parameters:

- Figure 4.a shows that the errors are larger with $h = 0.020$ than with $h = 0.039$, which appears to be more adapted to $\Delta x = 0.03125$ in this test. We can deduce from this (and from the fact that the above mesh size is too coarse - see subsection 3.1) that $\frac{h}{\Delta x} = \frac{0.039}{0.03125} = 1.248$ is the ideal Lagrangian-to-Eulerian mesh size ratio for our tool and for this test.
- The convergence of N_∞ while varying the timestep dt is of order $\sim$1.5 for $h = 0.039$ (in Figure 4.a, the slope for $h = 0.039$ is $\sim$1.5) and lower for $h = 0.02$. This lower convergence speed confirms the above conclusion about the optimal ratio $\frac{h}{\Delta x} = 1.248$.

4.3 Transient states results

We present in Figure 5a the Taylor parameter as a function of time for the Stokes flow and in Figure 5b for a Navier-Stokes computation with Reynolds number $Re = 10$. We see in Figure 5a a continuous decrease of $D_{1,2}$ under Stokes flow: in Figure 5b the influence of the inertial term appears through damped oscillations around the equilibrium state.

5 CONCLUSION

We have built and tested a tool which couples a finite volume fluid solver with a finite element solid solver using the Immersed Boundary Method. On a simple relaxation case, the coupled solver is shown to give satisfactory numerical precision under Stokes flow,

the timestep convergence being of the order 1.5. When comparing the capsule relaxation under Stokes and Navier-Stokes flow conditions, we find that oscillations in the capsule shape already occur for a flow Reynods Number of 10. The oscillations are due to inertia.

The numerical precision is comparable to that of classical methods, which shows that the immersed boundary method is adapted to solve transient problems. The present approach is also interesting for the advantages of the fluid solver itself. It is massively parallel (OpenMP and MPI) and can thus be used for large spatial simulations. Furthermore, the fluid solver also has an adaptative dynamic meshing that is useful to compute numerical solution near walls. Finally the viscosity and mass density can be changed dynamically, which is interesting to model solid or non-Newtonian cores for capsules flowing in a capillary. The novelty is that the fluid-structure code can resolve the flow of capsules of aspect ratios greater than 1 and non-zero Reynolds numbers, which are required to study capsules in microsystems. The fluid velocity field is also studied by considering the changes in the streamlines when varying the capillary number, which is crucial for the understanding of the fluid dynamics. The numerical model can be a useful complement to experimental measurements, as it provides local field quantities (fluid pressure and velocity, membrane tensions, ...), which cannot easily be evaluated experimentally, as well as information on topographic changes in streamlines. It thus provides useful additional information for the study of capsules in microsystems.

REFERENCES

[1] Johnston, A. P., Cortez, C., Angelatos, A. S. and Caruso, F. Layer-by-layer engineered capsules and their applications. *Curr. Opin. Colloid Interface Sci.* (2006) **11(4)**:203-209.

[2] Chang, K. S. and Olbricht, W. L. Experimental studies of the deformation and breakup of a synthetic capsule in extensional flow. *J. Fluid Mech.* (1993a) **250**:587-608.

[3] Chang, K. S. and Olbricht, W. L. Experimental studies of the deformation and breakup of a synthetic capsule in steady and unsteady simple shear flow. *J. Fluid Mech.* (1993b) **250**:609-633.

[4] Risso, F., Coll-Paillot, F. and Zagzoule, M. Experimental investigation of a bioartificial capsule flowing in a narrow tube. *J. Fluid Mech.* (2006) **547**:149-173.

[5] Barthès-Biesel, D. Motion of a spherical microcapsule freely suspended in a linear shear flow. *J. Fluid Mech.* (1980) **100**:831-853.

[6] Barthès-Biesel, D. and Rallison, J. M. The time-dependent deformation of a capsule freely suspended in a linear shear flow. *J. Fluid Mech.* (1981) **113**:251-267.

[7] Walter, J., Salsac, A.-V., Barthès-Biesel, D. and Le Tallec, P. Coupling of finite element and boundary integral methods for a capsule in a Stokes flow. *Int. J. Numer. Meth. Engng.* (2010) **83**:829-850.

[8] Wang, Z., Sui, Y., Salsac, A.-V. and Barthès-Biesel, D. Motion of a spherical capsule in branched tube flow with finite inertia. *J. Fluid Mech.* (2016) **806**:603-626.

[9] Tryggvason, G., Scardovelli, R. and Zaleski., S. *Direct Numerical Simulations of Gas-Liquid Multiphase Flows*. Cambrige Press University (2011)

[10] de Brauer, A., Iollo, A. and Milcent, T. A cartesian scheme for compressible multi-material models in 3D, *J. Fluid Mech.* (2016) **313**:121-143.

[11] Peskin, C.S. The immersed boundary method. *Acta Numerica* (2002) pp. 1-39.

[12] Beyer, R.P. and Leveque, R.J. Analysis of a One-Dimensional Model for the Immersed Boundary Method. *SIAM J. Numer. Anal.* (1992) **29(2)**:332-364.

[13] Balogh, P. and Bagchi, P. A computational approach to modeling cellular-scale blood flow in complex geometry. *J. Comput. Phys.* (2017) **334**:280-307.

[14] Popinet, S. Basilisk: simple abstractions for octree-adaptive scheme. *SIAM Conf on Para. Proc. for Sc. Comput.* (2016)

[15] Skalak, R., Tozeren, A., Zarda, R. P. and Chien, S. Strain energy function of red blood cell membranes. *Biophys. J.* (1973) **13**:245-264.

[16] Bell, J.B. and Collela, P. A Second-Order Projection Method for the Incompressible Navier-Stokes Equations in Arbitrary Domains. *J. Comput. Physics.* (1989) **85(2)**.

[17] Carroll, R. M. and Gupta, N. R. Inertial effects on the flow of capsules in cylindrical channels. *Int. J. Mult. Flow.* (2016) **87**:114-123.

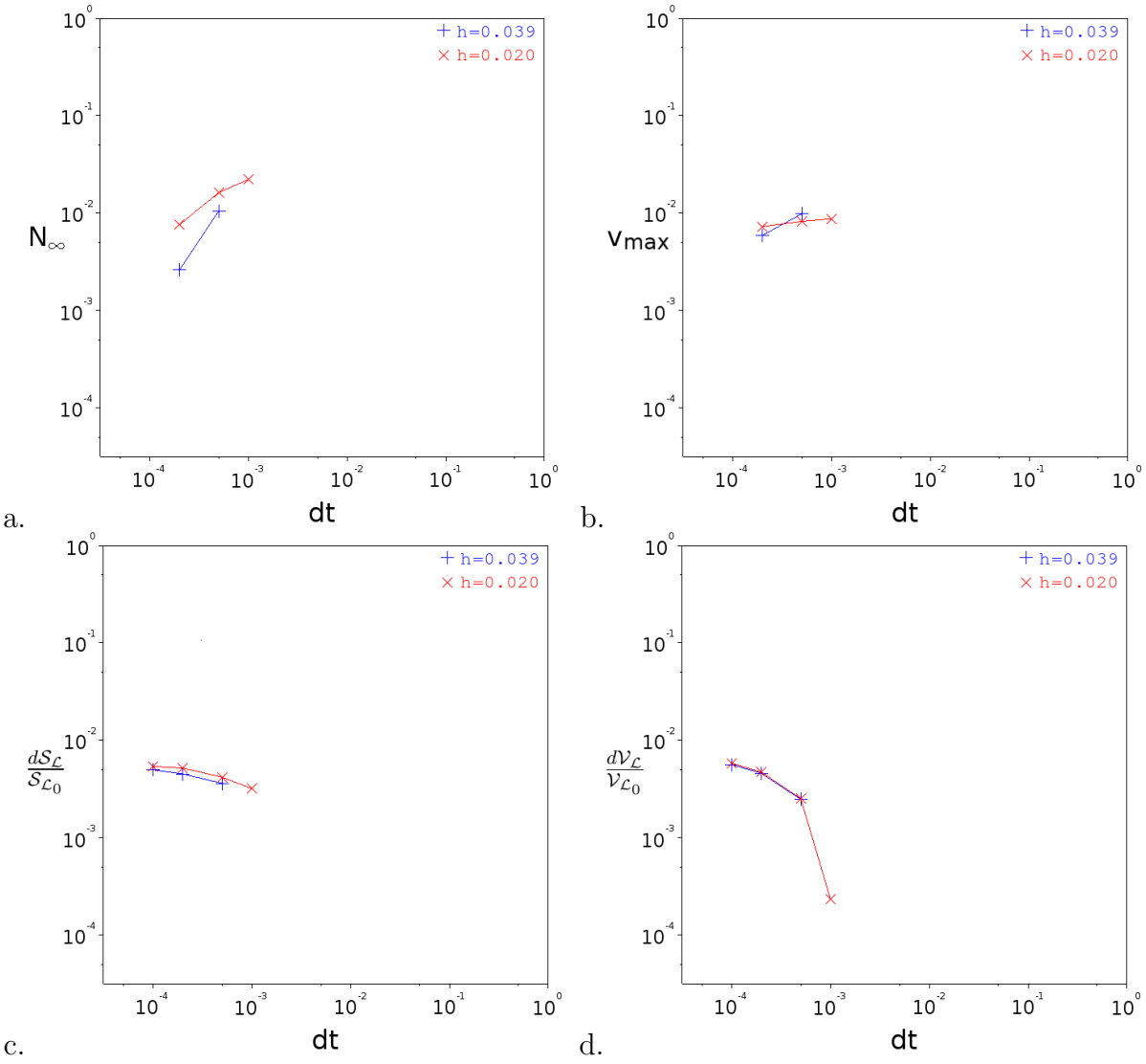

Figure 4: Convergence study: infinite norm error of the Lagrangian nodes positions to the case of the smallest timestep $dt_{\min} = 10^{-4}$ (a); Maximum speed norm in the fluid (b); Surface variation of the Lagrangian configuration compared to the reference spherical shape (c); Volume variation (d) (which is an error since it should be zero). Four different timesteps ($dt = 10^{-3}$, $dt = 5 \times 10^{-4}$, $dt = 2 \times 10^{-4}$, and $dt = 10^{-4}$) and two different Lagrangian meshes ($h = 0.039$ and $h = 0.020$) are tested.

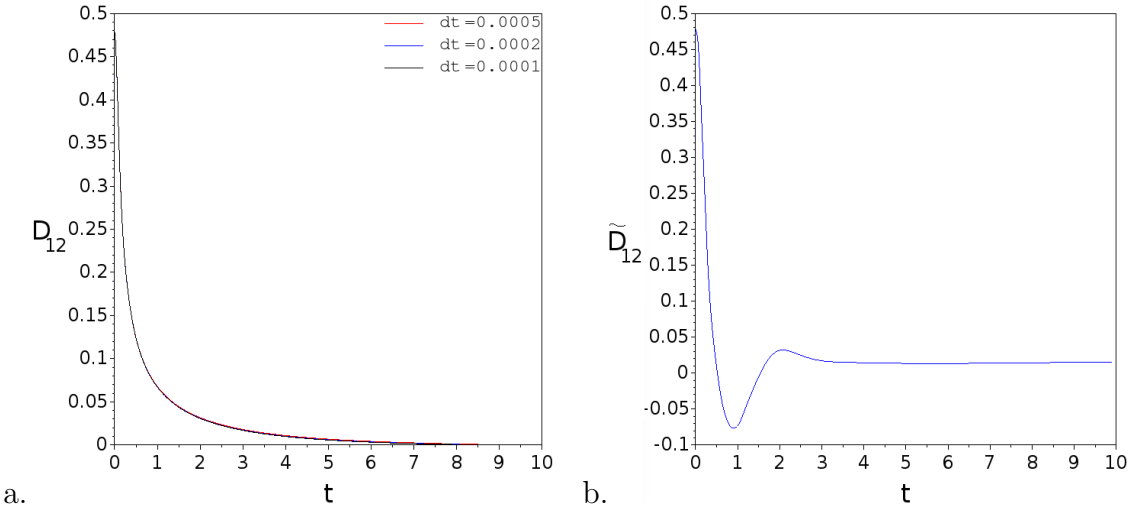

Figure 5: Time evolution of the Taylor parametrer (a) for Stokes flow and for a Navier-Stokes computation with $Re = 10$ (b).